ACS OMEGA

Open Access



http://pubs.acs.org/journal/acsodf

Article

# Development of Statistically Optimized Piperine-Loaded Polymeric Nanoparticles for Breast Cancer: In Vitro Evaluation and Cell Culture Studies

Sadaf Jamal Gilani,* May Nasser Bin-Jumah, and Farhat Fatima

Cite This: *ACS Omega* 2023, 8, 44183−44194

Read Online

ACCESS | Metrics & More | Article Recommendations | Supporting Information

**ABSTRACT:** Piperine (PPN) is a natural alkaloid derived from black pepper (*Piper nigrum* L.) and has garnered substantial attention for its potential in breast cancer therapy due to its diverse pharmacological properties. However, its highly lipophilic characteristics and poor dissolution in biological fluids limit its clinical application. Therefore, to overcome this limitation, we formulate and evaluate PPN-encapsulated polycaprolactone (PCL) nanoparticles (PPN-PCL-NPs). The nanoparticles were prepared by a single-step nanoprecipitation method and further optimized by a formulation design approach. The influence of selected independent variables PCL ($X_1$), poloxamer 188 (P-188; $X_2$), and stirring speed (SS; $X_3$) were investigated on the particle size (PS), polydispersity index (PDI), and % encapsulation efficiency (EE). The selected optimized nanoparticles were further assessed for stability, in vitro release, and in vitro antibreast cancer activity in the MCF-7 cancer cell line. The PS, PDI, zeta potential, and % EE of the optimized PPN-PCL-NPs were observed to be 107.61 ± 5.28 nm, 0.136 ± 0.011, −20.42 ± 1.82 mV, and 79.53 ± 5.22%, respectively. The developed PPN-PCL-NPs were stable under different temperature conditions with insignificant changes in their pharmaceutical attributes. The optimized PPN-PCL-NPs showed a burst release for the first 6 h and later showed sustained release for 48 h. The PPN-PCL-NPs exhibit exceptional cytotoxic effects in MCF-7 breast tumor cells in comparison with the native PPN. Thus, the formulation of PPN-loaded PCL-NPs can be a promising approach for better therapeutic efficacy against breast cancer.

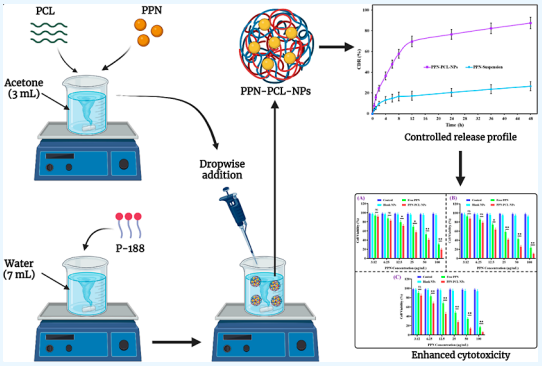


## 1. INTRODUCTION

Breast cancer (BC) is one of the most prevalent and deadly cancers worldwide, affecting millions of women and men yearly.[1] As per the GLOBOCON report of 2021, BC was diagnosed in 11.7% of all cases, establishing it as the most common form of cancer worldwide. It was closely followed by lung cancer at 11.4% and colorectal cancer at 10.0%.[2] Currently, chemotherapy stands as the primary treatment approach for BC.[3] However, severe adverse effects and the emergence of chemoresistance are the major concerns with conventional chemotherapy. Moreover, the lack of specificity to the tumor cells/tissues can kill the healthy cells in conventional chemotherapy of BC.[4] Therefore, selective delivery of chemotherapeutic drugs to the tumor cells/tissue becomes important to ensure the safe and effective treatment of BC. Additionally, most anticancer molecules are highly lipophilic in nature and show poor solubility in biological fluids and limited bioavailability.[5,6] Therefore, a novel approach is required to overcome the limitations of conventional chemotherapy to prevent and treat BC.

Among the plethora of bioactive compounds, piperine (PPN), a natural alkaloid derived from black pepper (*Piper nigrum* L.), has garnered substantial attention for its potential in BC therapy.[7,8] PPN acts by targeting numerous signaling pathways via the following mechanisms: (i) induction of apoptosis and cell cycle arrest; (ii) modulation in expression of signaling proteins, caspase 3, 8, and 9; (iii) reduction in transcription factor like NF-κB; and (iv) tumor growth inhibition by affecting the tumor microenvironment.[9,10] Moreover, its favorable safety profile and natural origin make it an appealing candidate for further investigation as an adjuvant in BC therapy.[11,12] PPN belongs to the biopharmaceutical classification system (BCS) "class II" compound which means it has low solubility and high permeability.[13] In a study, Suresh and Srinivasan investigated the pharmacokinetic parameters after oral administration (170 mg/kg) in rats. The highest concentration of PPN was achieved at 1 h, and only 10.8% of PPN was observed after 6 h. The plasma half-life of PPN was observed to be 18.2 h.[14] PPN is characterized by high

Received: September 2, 2023
Revised: October 21, 2023
Accepted: October 24, 2023
Published: November 9, 2023

lipophilicity (log $P$ = 2.25) and poor aqueous solubility (22.34 mg/L at 25 °C).[15] These physicochemical properties are responsible for the poor pharmacokinetic profile of PPN due to slow absorption and low oral bioavailability.[16] Hence, there is an immediate requirement to develop a novel and effective delivery system that can enhance bioavailability and thereby therapeutic efficacy of encapsulated compounds.

By developing nanoparticle-based drug delivery systems, the above-discussed challenges can be addressed. Nanoparticles (NPs) show significantly higher surface area due to nanometric size (<200 nm) and spherical morphology that enhanced the absorption, thereby, bioavailability of the encapsulated drug.[17] Encapsulation of lipophilic compounds in the nanoparticles significantly increases the solubility, stability, and dissolution in the biological fluids.[17] Further, the NP-based system represents several advantages over conventional drug delivery systems, such as enhanced permeability and retention (EPR) effect, improved solubility and stability of anticancer compounds, and reduced dose-related toxicity.[18,19] In this context, Pachauri et al. prepared PPN-loaded PEG−PLGA nanoparticles for enhanced therapeutic efficacy against BC.[20] The developed nanoparticles showed favorable pharmaceutical attributes like small particle size (PS; 131.4 ± 6.6 nm), polydispersity index (PDI; 0.037 ± 0.021), and satisfactory encapsulation efficiency (% EE; >35%). Moreover, the developed PPN-loaded nanocarrier exhibited significantly higher cellular uptake and anticancer effects against MCF-7 cells than native PPN. Similarly, Kazmi et al. prepared PPN-encapsulated lipid-polymer hybrid nanoparticles (PPN-LPHNPs) to achieve higher therapeutic efficacy against BC.[21] The developed PPN-LPHNPs showed a PS, PDI, and % EE of 151.2 ± 4.12 nm, 0.213 ± 0.02, and 83.54 ± 2.88%, respectively. Further, the nanocarrier showed a lower $IC_{50}$ value in the cell viability study using MCF-7 cells than pure PPN. However, the therapeutic efficacy of PPN-loaded polycaprolactone (PCL) nanoparticles has never been investigated against BC.

PCL is a synthetic biodegradable polymer that has been widely employed in the development of NPs for anticancer drug delivery. PCL-NPs offer several advantages, including controlled release of encapsulated drugs, prolonged circulation time, and ease of preparation.[22,23] It is nontoxic in nature and cytocompatibility makes it an ideal material for drug delivery.[24] These characteristics, along with its excellent permeability to various compounds with relatively low molecular weights (<400 Da), make PCL a suitable polymer for the development of nanoparticles.[25] Further, the formulation of these stable nanoparticles by using poloxamers can protect the encapsulated compound from premature degradation and facilitate their controlled release at the tumor site.[26] Poloxamers belong to the class of synthetic triblock copolymers. They consist of central hydrophobic poly(propylene oxide) chains enveloped by two hydrophilic poly(ethylene oxide) chains. Their favorable physicochemical properties and excellent biocompatibility make the poloxamer a promising candidate to fabricate stable nanoparticles for drug delivery. Furthermore, their amphiphilic characteristics and the capability to self-assemble into micelles make them ideal materials for developing nanoparticles.[27,28]

Therefore, we aimed to develop PPN-encapsulated PCL nanoparticles for BC therapy. We hypothesized that PCL nanoparticles would improve the physicochemical properties and biological performance of PPN by increasing their solubility, stability, and cellular uptake. Herein, the PPN-PCL-NPs were prepared by a nanoprecipitation technique and optimized by a $3^3$-Box−Behnken design ($3^3$-BBD) and thereafter characterized for different pharmaceutical attributes. The storage stability under different temperature conditions and in vitro drug release was further conducted. Further, the cellular uptake, as well as the cytotoxic potential of the developed nanoparticles in MCF-7 BC cells, was investigated.

## 2. MATERIALS AND METHODS

**2.1. Materials.** PPN (>97% purity), polycaprolactone (PCL; MW = 45 kDa), and dialysis bag (MWCO: 12 kDa) were obtained from Sigma-Aldrich located in St. Louis, MO, USA. BASF, Mumbai, India generously provided poloxamer-188 (P-188). Acetone was acquired from Merck, Mumbai, India. Fetal bovine serum (FBS), paraformaldehyde, penicillin, streptomycin, and dimethyl sulfoxide (DMSO) were all purchased from Thermo Fisher Scientific, New Delhi, India. MCF-7 cell lines were sourced from the National Centre for Cell Science (NCCS), Pune, India. Any other chemicals utilized in the present investigation were of high purity and belonged to analytical grade.

**2.2. Box−Behnken Experimental Design.** To develop optimized PPN-PCL-NPs, we employed a $3^3$-BBD by utilizing Design-Expert software V.13.0 (State Ease Inc., Minneapolis, USA). During the initial investigation, we selected three independent variables: the concentration of polycaprolactone (PCL; $X_1$), the concentration of poloxamer 188 (P-188; $X_2$), and the stirring speed (SS; $X_3$). These factors were assessed at three levels: high ("+1"), medium ("0"), and low ("−1"). The impact of these independent variables on three dependent factors, i.e., PS ($Y_1$), PDI ($Y_2$), and % EE) ($Y_3$) was evaluated as documented in Table 1. By fitting the data into the $3^3$-BBD, the design derived 15 excipient compositions for PPN-PCL-NP development. Subsequently, we developed all 15 PPN-PCL-NPs according to their compositions, and the resulting values are documented in Table 2. Afterward, various statistical models, including linear, 2-F1, and quadratic models, were examined to identify the most fitting data by employing one-way analysis of variance (ANOVA). The chosen model was then elucidated using a polynomial equation, and the software generated various plots to illustrate the model's behavior.

**Table 1. Chosen Independent and Dependent Factors Used in the $3^3$-BBD for PPN-PCL-NP Development**

| factor (independent variable) | levels | | |
|---|---|---|---|
| independent variables | low (−1) | medium (0) | high (+1) |
| $X_1$ = concentration of PCL (mg) | 40 | 60 | 80 |
| $X_2$ = concentration of P-188 (%) | 0.5 | 0.75 | 1 |
| $X_3$ = stirring speed (rpm) | 600 | 900 | 1200 |
| responses (dependent variables) | | goal | |
| $Y_1$ = particle size (PS; nm) | | minimize | |
| $Y_2$ = polydispersity index (PDI) | | minimize | |
| $Y_3$ = encapsulation efficiency (EE; %) | | maximize | |

**2.3. PPN-PCL-NP Preparation.** PPN-PCL-NPs were prepared using a nanoprecipitation method, slightly modified from previously documented techniques.[29,30] Initially, an aqueous surfactant solution was prepared by dissolving P-188 (0.5−1% w/v) in 7 mL of Milli-Q water. Separately, PCL (40−80 mg) and 20 mg of PPN were dissolved in acetone (3 mL) to make an organic solution by constant stirring. Subsequently, the organic phase was gradually added drop-by-drop into the surfactant solution using a 1 mL syringe under continuous


https://doi.org/10.1021/acsomega.3c06605
ACS Omega 2023, 8, 44183−44194

Table 2. Experimental Compositions Derived from $3^3$-BBD for PPN-PCL-NP Preparation with Values of $Y_1$ (PS), $Y_2$ (PDI), and $Y_3$ (% EE)

| | independent factors | | | dependent factors (responses) | | |
|---|---|---|---|---|---|---|
| runs | $X_1$ (mg) | $X_2$ (%) | $X_3$ (rpm) | $Y_1$ (PS in nm) | $Y_2$ (PDI) | $Y_3$ (EE in %) |
| F1 | 80 | 0.5 | 900 | 136.10 | 0.197 | 76.72 |
| F2 | 80 | 0.75 | 1200 | 116.91 | 0.191 | 82.94 |
| F3 | 40 | 0.75 | 1200 | 82.07 | 0.134 | 63.57 |
| F4 | 80 | 0.75 | 600 | 127.20 | 0.157 | 87.14 |
| F5 | 40 | 0.75 | 600 | 98.63 | 0.106 | 72.61 |
| F6 | 60 | 0.5 | 1200 | 107.64 | 0.181 | 64.75 |
| F7 | 60 | 0.75 | 900 | 110.56 | 0.138 | 76.82 |
| F8 | 40 | 0.5 | 900 | 104.69 | 0.135 | 62.85 |
| F9 | 60 | 0.75 | 900 | 109.42 | 0.143 | 82.27 |
| F10 | 60 | 1 | 600 | 109.13 | 0.136 | 79.60 |
| F11 | 80 | 1 | 900 | 124.43 | 0.176 | 89.19 |
| F12 | 60 | 1 | 1200 | 97.14 | 0.165 | 73.58 |
| F13 | 40 | 1 | 900 | 91.51 | 0.127 | 68.65 |
| F14 | 60 | 0.5 | 600 | 125.41 | 0.149 | 71.92 |
| F15 | 60 | 0.75 | 900 | 107.81 | 0.135 | 80.67 |

stirring (SS; 600−1200 rpm). The obtained amalgamation was continuously stirred for 3 h to enable the self-assembly of PPN-PCL-NPs. Lastly, the produced PPN-PCL-NPs were subjected to dialysis for 12 h against Milli-Q water to eliminate the organic solvent to obtain the final nanocarrier.

**2.4. PPN-PCL-NP Characterization.** *2.4.1. Particle Size Distribution and Zeta Potential Measurement.* The size distribution (i.e., PS and PDI) and zeta potential (ZP) of PPN-PCL-NPs were measured by the principle of dynamic light scattering by using a Zetasizer (Nano-ZS, Malvern Instruments Inc., UK). In brief, a 0.2 mL aliquot of PPN-PCL-NPs was diluted with Milli-Q water to 3 mL, and the samples were positioned in the zeta cuvette. Finally, the zeta analysis was conducted at a 90° scattering angle.

*2.4.2. Morphology of PPN-PCL-NPs.* The morphology analysis of the developed PPN-PCL-NPs was conducted by using a transmission electron microscope (TEM; JEM-1200EX, JEOL, Japan). A drop of PPN-PCL-NPs was placed onto a 300-mesh copper grid and negatively stained using 1% phosphotungstic acid. Subsequently, the grid was allowed to air-dry and was visualized under a TEM. The microscope was operated at a voltage of 200 kV and 5000$x$/5000× magnification to achieve point-to-point resolution.

*2.4.3. Encapsulation Efficiency (% EE) and Drug Loading (% DL).* The determination of % EE and % DL for PPN-PCL-NPs was conducted by an indirect methodology as reported in a previous protocol.[31,32] In accordance with this protocol, PPN-PCL-NPs were subjected to centrifugation at 15,000 rpm for a duration of 20 min, by employing a cooling centrifuge (Remi, Mumbai, India). Subsequent to centrifugation, the resulting supernatant was isolated and subjected to filtration with a 0.22 $\mu$m nylon filter. The quantification of unencapsulated PPN present within the filtrate was subsequently performed utilizing a UV-spectrophotometer (Shimadzu, UV-1800 model, Kyoto, Japan) at a wavelength of 342 nm (validation details explained in Supporting Information). Finally, the % EE and % DL were subsequently calculated by the following formulas.

$$\%\ \text{EE} = \frac{\text{total PPN} - \text{unentrapped PPN}}{\text{total PPN}} \times 100 \quad (1)$$

$$\%\ \text{DL} = \frac{\text{total PPN} - \text{unentrapped PPN}}{\text{weight of PCL} - \text{NPs}} \times 100 \quad (2)$$

**2.5. Stability Study.** Stability is a crucial aspect in the formulation of pharmaceutical products. Ensuring the safety, effectiveness, and quality of pharmaceutical products is imperative for their approval and acceptance. Therefore, an evaluation of the storage stability was conducted for the optimized PPN-PCL-NPs (5 mL). PPN-PCL-NPs (5 mL) were placed in glass vials and subjected to storage at controlled temperatures: 5 ± 1, 25 ± 2, and 40 ± 2 °C, spanning a duration of 3 months in a stability chamber (Weiss Envirotronics, Michigan, USA).[33,34] Changes in PS, PDI, ZP, and % EE of the PPN-PCL-NPs were monitored every 15 days throughout the 3 month period.

**2.6. In Vitro Drug Release.** The in vitro release pattern of PPN-encapsulated PCL-NPs was assessed by dialysis bag technique, following previously established protocols.[35,36] Initially, the dialysis bag was soaked in distilled water for 12 h. Subsequently, 2 mL of PPN-PCL-NPs, equivalent to 4 mg of PPN, was poured into the dialysis bag, and both ends were securely fastened using a commercial thread. The dialysis bag was then submerged in a beaker bearing 500 mL of phosphate buffer at pH 7.4 with Tween 80 (0.5%). The experiment was conducted at a temperature of 37 ± 1 °C with continuous stirring at a speed of 100 rpm. Over predecided time periods, 2 mL samples were withdrawn from the releasing media, and an equivalent volume of neat media was replenished to maintain a consistent sink condition. Lastly, the released PPN was assessed by employing a UV-spectrophotometer at 342 nm wavelength (validation details explained in the Supporting Information). The validation parameters of the drug are shown in Tables S1 and S2. To assess the PPN release mechanism from the PCL-NPs, the release data obtained from PPN-PCL-NPs were applied to various kinetic models, including zero-order, first-order, Higuchi, and Korsmeyer−Peppas models. The mathematical model demonstrating the correlation coefficient ($R^2$) closest to 1 was identified as the most suitable fit model.[37]

**2.7. Cell Culture Experiments.** An MCF-7 cell line was employed for investigating the cytotoxicity. These cells were cultured in Dulbecco's modified Eagle's medium, supplemented with L-glutamine and antibiotics such as streptomycin and penicillin, and the temperature was maintained at 37 °C, under a humidified atmosphere with 5% $CO_2$ and 95% air. To supplement the MCF-7 cells, 10% heat-inactivated FBS was also added. Experiments were performed only when the confluency of cells reached ∼80%. The cytotoxicity evaluation of free PPN and PPN-PCL-NPs was conducted by the MTT assay, as previously reported[38,39] in the MCF-7 cell line. Concisely, the MCF-7 cells were seeded in 96-well plates at a density of 1 × $10^5$ cells per well and cultured for 24 h. Subsequent to achieving confluence, the cells were subjected to various concentrations of PPN-PCL-NPs and free PPN. The treated cells were then incubated within a $CO_2$ incubator for durations of 24, 48, and 72 h. At the culmination of each respective incubation period, a solution of MTT dye (25 $\mu$L), having a 0.5 mg/mL concentration, was supplemented to each well plate. This was followed by an additional 4 h of incubation to facilitate the formation of formazan crystals. Following this incubation, the excess culture medium was discarded and the formazan crystals were dissolved utilizing 100 $\mu$L of DMSO. To ensure complete dissolution, the plates were gently agitated on a shaker for 30 min. Ultimately, the optical density of the dissolved


https://doi.org/10.1021/acsomega.3c06605
ACS Omega 2023, 8, 44183−44194

**Table 3. Regression Analysis Data for Dependent Variables after Fitting the Data into Different Mathematical Models**

| model | $R^2$ | adjusted $R^2$ | predicted $R^2$ | SD | press | remark |
|---|---|---|---|---|---|---|
| | | | Response 1 ($Y_1$) | | | |
| linear | 0.9476 | 0.9332 | 0.8894 | 3.74 | 323.78 | |
| 2F1 | 0.9540 | 0.9194 | 0.7620 | 4.11 | 696.76 | |
| quadratic | 0.9981 | 0.9948 | 0.9882 | 1.04 | 34.59 | Suggested |
| | | | Response 2 ($Y_{2)}$ | | | |
| linear | 0.8851 | 0.8538 | 0.8109 | 0.0099 | 0.0018 | |
| 2F1 | 0.8913 | 0.8098 | 0.6602 | 0.0113 | 0.0032 | |
| quadratic | 0.9964 | 0.9899 | 0.9904 | 0.0026 | 0.0001 | Suggested |
| | | | Response 3 ($Y_{3)}$ | | | |
| linear | 0.8556 | 0.8162 | 0.7662 | 3.55 | 224.50 | |
| 2F1 | 0.8736 | 0.7788 | 0.6442 | 3.90 | 341.70 | |
| quadratic | 0.9832 | 0.9530 | 0.9563 | 1.80 | 42.01 | Suggested |

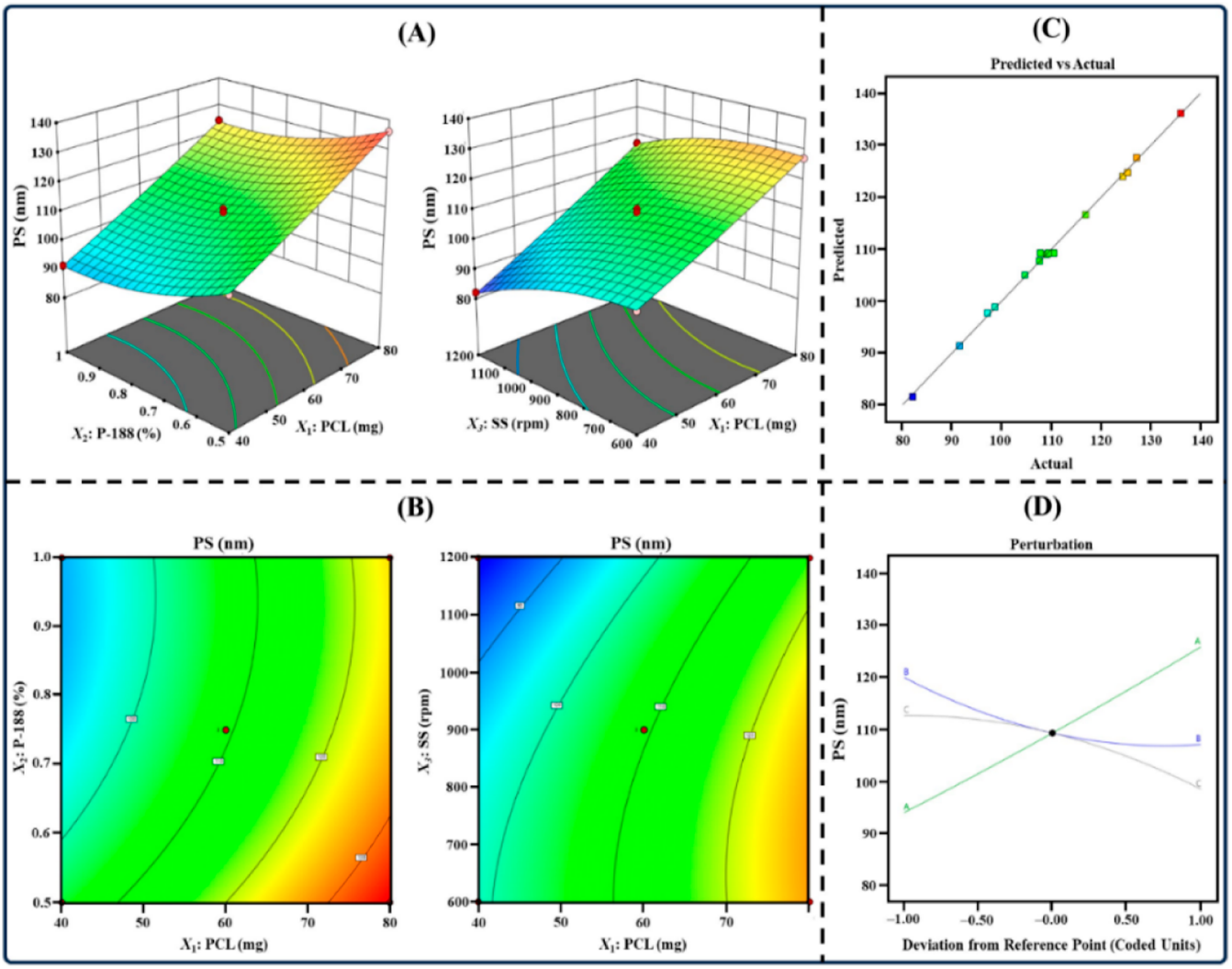


**Figure 1.** Different response plots generated from $3^3$-BBD. (A) 3D surface, (B) contour, (C) predicted vs actual, and (D) perturbation plots representing the influence of independent factors on PS of PPN-PCL-NPs.

formazan was quantified using a plate reader (BioTek, Winooski, USA) at a 570 nm wavelength.

**2.8. Data Analysis.** For data analysis, we employed GraphPad Prism, Version 8 software. The experimental protocols were replicated three times, and the outcomes have been presented as the arithmetic mean ± standard deviation. To determine significant distinctions between the groups, a two-tailed Student's *t*-test was employed. Statistical significance was acknowledged if the computed *p*-value stood below 0.05.

## 3. RESULTS AND DISCUSSION

**3.1. Preparation and Optimization by Experimental Design.** Herein, the PPN-PCL-NPs were formulated by a single-step nanoprecipitation method. This method is widely used and considered to be the most reliable for developing small-



https://doi.org/10.1021/acsomega.3c06605
ACS Omega 2023, 8, 44183−44194

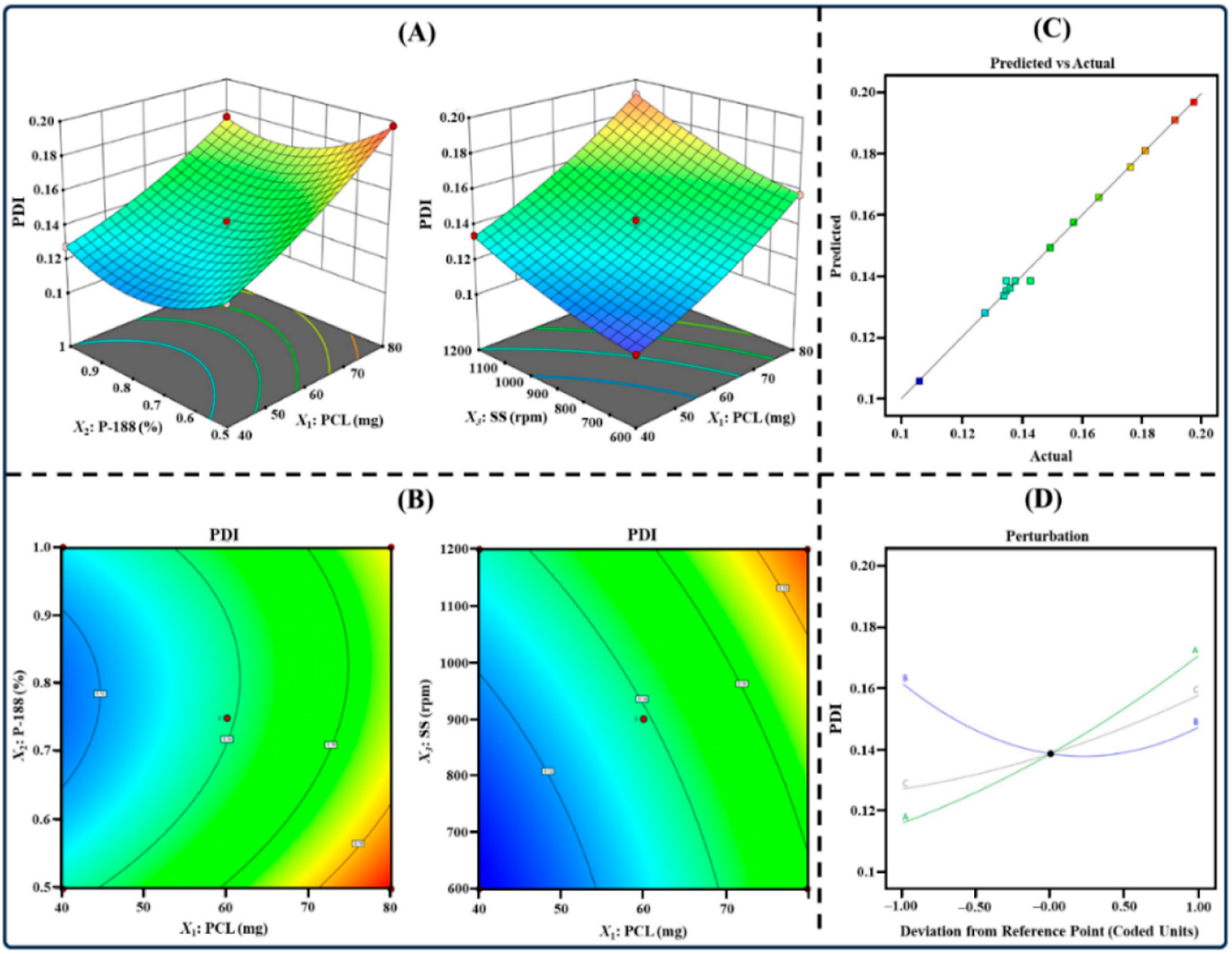


**Figure 2.** Different response plots generated from $3^3$-BBD. (A) 3D surface, (B) contour, (C) predicted vs actual, and (D) perturbation plots representing the influence of independent factors on the PDI of PPN-PCL-NPs.

sized PLHNPs (generally <150 nm) with a high production yield. The pharmaceutical attributes of the developed PCL-NPs are highly dependent on the polymer and surfactant, and stirring speed for mixing of the solution. All 15 PPN-PCL-NPs were developed according to the composition derived from the $3^3$-BBD, and the values of responses were fitted into the software to yield the final excipient composition (Table 2).

The responses were separately accommodated within different statistical models through linear regression analysis to determine the most suitable model exhibiting the highest adjusted and predicted $R^2$ values (Table 3). Subsequent identification of significant terms impacting the responses was carried out utilizing ANOVA analysis. When the *p*-value was observed to be < 0.05, the terms were considered as statistically significant within the model. The ANOVA analysis for each response yielded a value of $P < 0.0001$. According to the output as represented in Table 3, the quadratic model exhibits the highest adjusted and predicted $R^2$ value, which was closest to 1, hence considered the best-fit model for all responses. To comprehend the effect of independent factors on each response, three-dimensional (3D) surface plots, contour plots, and perturbation plots were generated. Additionally, the secondary polynomial equations for each response were generated from the design to examine the impact of independent factors. The secondary polynomial equations for all the three responses obtained from the design are as follows

$$\text{Particle size(PS)} = +109.26 + 15.97X_1 - 6.46X_2 - 7.08X_3 + 0.3760X_1X_2 + 1.57X_1X_3 + 1.44X_2X_3 + 0.6460X_1^2 + 4.27X_2^2 - 3.71X_3^2 \quad (3)$$

$$\text{Polydispersity index(PDI)} = +0.1387 + 0.0274X_1 - 0.0071X_2 + 0.0154X_3 - 0.0035X_1X_2 + 0.0014X_1X_3 - 0.0005X_2X_3 + 0.0047X_1^2 + 0.0158X_2^2 + 0.0038X_3^2 \quad (4)$$

$$\text{Entrapment efficiency(\% EE)} = +79.92 + 8.54X_1 + 4.35X_2 - 3.30X_3 + 1.67X_1X_2 + 1.21X_1X_3 + 0.2866X_2X_3 - 0.7333X_1^2 - 4.83X_2^2 - 2.62X_3^2 \quad (5)$$

*3.1.1. Impact of Dependent Factors on PS ($Y_1$).* Herein, the PS range of the PPN-PCL-NPs spanned from 91.51 to 136.10 nm, suggesting the successful formation of PCL-NPs with small


https://doi.org/10.1021/acsomega.3c06605
ACS Omega 2023, 8, 44183−44194

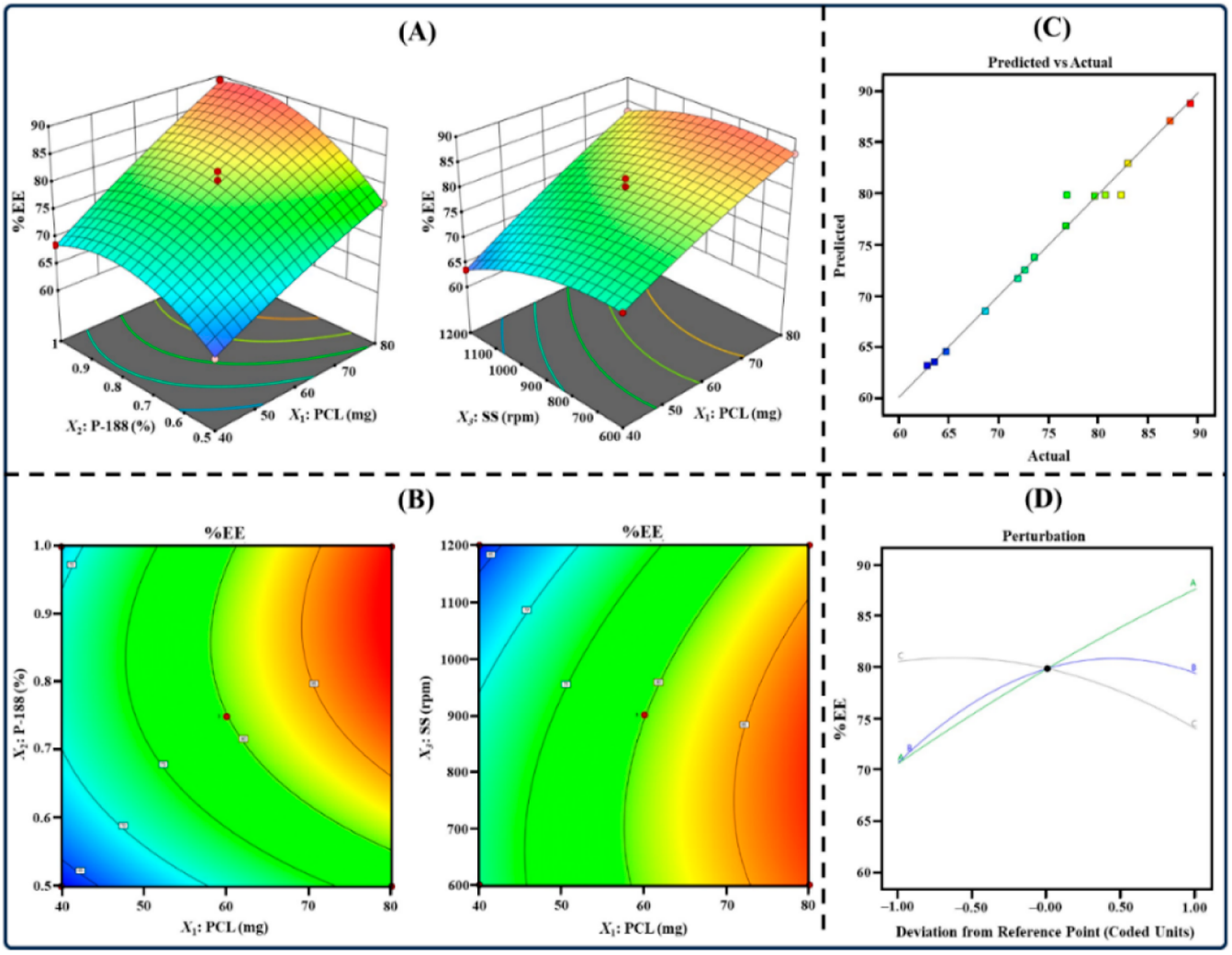


**Figure 3.** Different response plots generated from $3^3$-BBD. (A) 3D surface, (B) contour, (C) predicted vs actual, and (D) perturbation plots representing the influence of independent factors on % EE of PPN-PCL-NPs.

dimensions (<150 nm). ANOVA unveiled the substantial influence of independent factors i.e., PCL concentration, P-188 concentration, and stirring speed on the mean PS ($p < 0.0001$). Examination of response plots, as depicted in Figure 1, and polynomial eq 3 suggested that elevating the PCL quantity from 40 to 80 mg resulted in a significant increase in the size of PPN-PCL-NPs. This substantial rise in the PS is attributed to the increment in PCL quantity that enhances the viscosity of the organic solution. The increased viscosity, in turn, reduces the shear efficiency which is crucial for particle breakdown during the preparation process.[40,41] Conversely, augmenting the P-188 concentration from 0.5 to 1% (w/v) induced a marked reduction in the PS of PPN-PCL-NPs. Such an effect was achieved due to the high P-188 concentration present at the organic/water interface during the emulsification process, fostering the fabrication of small-sized PPN-PCL-NPs. Further, the reduced interfacial tension is facilitated by the increased P-188 concentration during the PCL-NP preparation, which, in turn, contributes to the reduction in PS.[42,43] Likewise, an appreciable decrease in the PS of PPN-PCL-NPs was observed on increasing the stirring speed (SS; $X_3$) from 600 to 1200 rpm. The intensity of shear stress bears an indirect relationship with PS, wherein heightened shear stress is correlated with diminished PS. Elevated stirring speed imparts greater energy into the process, thereby engendering PPN-PCL-NPs characterized by smaller PS.[44]

*3.1.2. Impact of Dependent Factors on the PDI ($Y_2$).* Herein, the PDI range of the PPN-PCL-NPs spanned from 0.106 to 0.197, indicating the successful formation of nanoparticles characterized by excellent homogeneity (PDI < 0.2). ANOVA unveiled the substantial influence of independent factors i.e., PCL concentration, P-188 concentration, and stirring speed on the mean PDI ($p < 0.0001$). Evaluation of the response plots, as depicted in Figure 2, and polynomial eq 4 elucidated that augmenting the PCL quantity from 40 to 80 mg led to a substantial increase in the PDI of the PPN-PCL-NPs. A significant increase in the PDI is ascribed to the gradual increment in the viscosity of the organic phase. The augmented viscosity, in turn, contributes to an increment in the heterogeneity between the particles, thereby yielding PCL-NPs characterized by higher PDI values.[45] Conversely, a notable reduction in the PDI of PPN-PCL-NPs was evident with an increase in P-188 quantity from 0.5 to 1% w/v. The gradual augmentation in the P-188 concentration significantly decreased the interfacial tension, thereby enhancing the emulsification and promoting the formation of small-sized particles with exceptional uniformity.[46] Meanwhile, a modest increment in the stirring speed from 600 to 1200 rpm yielded a moderate rise in


https://doi.org/10.1021/acsomega.3c06605
ACS Omega 2023, 8, 44183−44194

**Table 4. Summary of the Optimized Independent Factors and Dependent Factors of the Optimized PPN-PCL-NPs**

| independent factors | | | dependent factors | | |
|---|---|---|---|---|---|
| PCL (mg) | P-188 (%) | SS (rpm) | PS (nm) | PDI | % EE |
| 60 | 0.75 | 900 | 107.61 ± 5.28 | 0.136 ± 0.011 | 79.53 ± 5.22 |

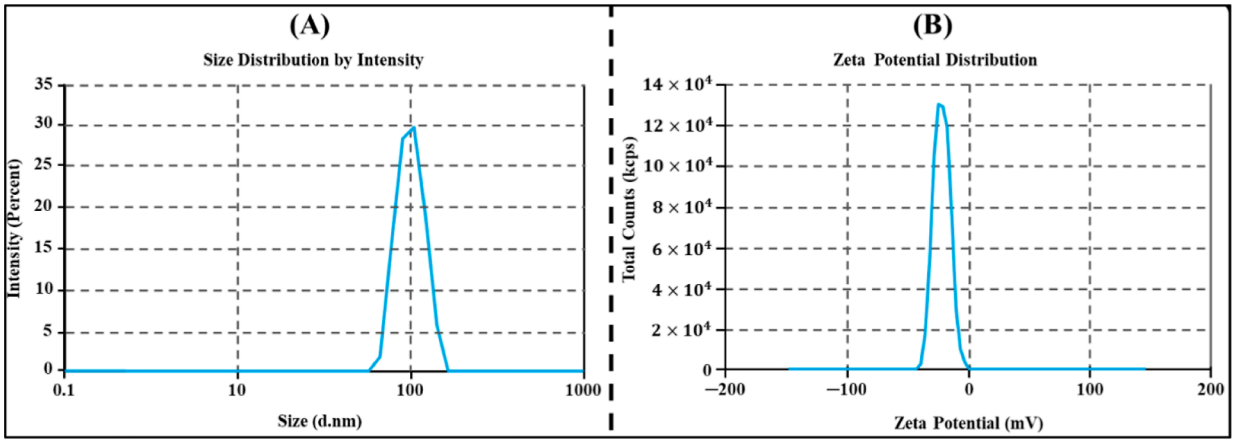


**Figure 4.** Plots depicting (A). Particle size distribution and (B). ZP of the optimized PPN-PCL-NPs.

the PDI of PPN-PCL-NPs. An increase in PDI on increasing SS ($X_3$) from 900 to 1200 rpm is ascribed to an increase in shear energy that produces NPs with high surface charge that leads to the coagulation of NPs.[47]

*3.1.3. Impact of Dependent Factors on % EE ($Y_3$).* Herein, the % EE range of the PPN-PCL-NPs spanned from 62.85 to 89.19%, indicative of the successful development of nanoparticles with excellent encapsulation efficiency. ANOVA unveiled the substantial influence of independent factors i.e., PCL concentration, P-188 concentration, and stirring speed on the mean % EE ($p < 0.0001$). Evaluation of the response plots, as depicted in Figure 3, and polynomial eq 5 elucidated that increasing the PCL quantity from 40 to 80 mg resulted in a considerable enhancement in the % EE of the PPN-PCL-NPs. This marked elevation in % EE associated with increased PCL concentration can be attributed to the increased space provided by the polymer for encapsulating PPN. Consequently, a relatively compact matrix is formed, facilitating more efficient drug encapsulation.[41] Similarly, increasing the P-188 quantity from 0.5 to 1% w/v resulted in an increase in the % EE of nanoparticles. This phenomenon is attributed to the enhanced emulsification resulting from an increased surfactant concentration, which in turn leads to a substantial increment in the % EE of the nanoparticles. Conversely, the % EE of PPN-PCL-NPs was significantly reduced upon increasing the stirring speed from 600 to 1200 rpm. This outcome can be attributed to the increased SS ($X_3$) causing a reduction in PS, which in turn contributes to a decrease in % EE.[44]

*3.1.4. Selection of Optimized PPN-PCL-NPs.* The selection of the optimal composition for the formulation of PPN-PCL-NPs was made on a desirability approach from the $3^3$-BBD. The main objective was formulating the PPN-PCL-NPs with small PS and PDI with high % EE. The PPN-PCL-NPs prepared with 60 mg of PCL, 0.75% (w/v) P-188, and 900 rpm stirring speed fulfilled the criteria. Interestingly, the optimized PPN-PCL-NPs exhibited an aggregate desirability value of 0.941, close to 1. This value signifies a robust methodological approach. Subsequent to this, three distinct formulations were selected based on the optimized composition. The results of the optimized PPN-PCL-NPs are summarized in Table 4.

**3.2. PPN-PCL-NP Characterization.** *3.2.1. PS, PDI, and ZP Measurement.* The mean PS of nanocarriers significantly impacts cellular internalization, the duration of systemic circulation, and clearance dynamics. Moreover, nanocarriers possessing a PS below 200 nm tend to translocate in solid tumors.[48] Herein, the mean PS of the optimized PPN-PCL-NPs was found to be 107.61 ± 5.28 nm, as shown in Figure 4A. The PDI serves as a metric for assessing the size distribution of the nanoparticle populations within a system. Ranging from 0 to 1, the PDI value characterizes the extent of dispersion quality, with values ≤ 0.1 signifying optimal homogeneity. However, a PDI value ≤ 0.5 is often considered satisfactory by researchers.[49] Notably, this investigation ascertained a PDI value of 0.136 ± 0.011 for the optimized PPN-PCL-NPs, thus implying excellent homogeneity. The ZP serves as a critical parameter for delineating the surface charge of nanocarriers and exerts a pivotal influence on their stability. Higher positive or negative ZP results in robust repulsive interactions among nanoparticles, indicative of better stability.[30] Illustrated in Figure 4B, the ZP values for the optimized PPN-PCL-NPs showed a value of −20.42 ± 1.82 mV. A high negative charge on the surface of nanocarriers is attributed to the carboxylic groups in PCL and the presence of P-188, serving as an emulsifier.[46]

*3.2.2. Morphology of PPN-PCL-NPs.* The morphology assessment of PPN-PCL-NPs was conducted by using TEM, as shown in Figure 5. The TEM micrograph distinctly unveiled the spherical shape of PPN-PCL-NPs, characterized by smooth and well-defined surfaces. The PS of PPN-PCL-NPs observed through TEM corresponded well with the outcomes derived from the Zetasizer analysis. The geometric configuration of nanocarriers plays a pivotal role in modulating their cellular uptake and biodistribution.[50] Interestingly, spherical nanoparticles hold significant importance due to their versatile attributes, encompassing elevated surface-to-volume ratios and distinct optical properties. Spherical nanoparticles are particularly favored due to their improved individual cellular uptake, which in turn augments therapeutic efficacy.[51]


https://doi.org/10.1021/acsomega.3c06605
ACS Omega 2023, 8, 44183−44194

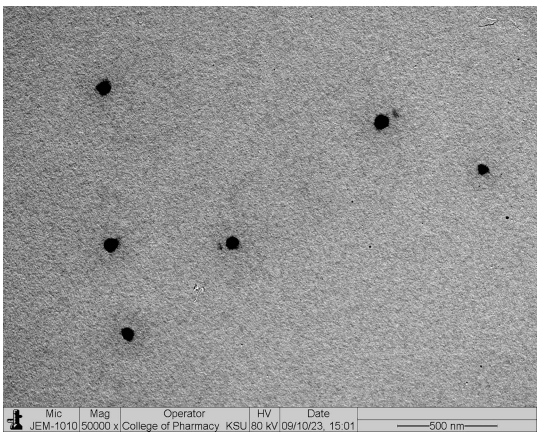


**Figure 5.** TEM micrograph of optimized PPN-PCL-NPs.

*3.2.3. % EE and % DL.* % EE and % DL are crucial parameters that can significantly impact the effectiveness and potential applications of the nanoparticles. The % EE and % DL of the optimized PPN-PCL-NPs were observed to be 79.53 ± 5.22, and 7.26 ± 1.33%, respectively. Overall, satisfactory % EE and % DL were ascertained owing to the robust polymeric matrix of the nanoparticles.

**3.3. Stability Study.** The stability of optimized PPN-PCL-NPs was determined based on their changes in PS, PDI, % EE, and ZP when stored under different temperature conditions. Changes in different physicochemical parameters of PPN-PCL-NPs with respect to the different temperature conditions are shown in Figure 6. The PPN-PCL-NPs exhibited exceptional stability at 5 ± 1 °C with minor modulation of the physicochemical parameters. Likewise, only insignificant alteration in the physicochemical parameters of PPN-PCL-NPs was ascertained at a 25 ± 2 °C temperature. Nevertheless, at 40 ± 2 °C, significant alterations in the physicochemical parameters of PPN-PCL-NPs were ascertained. A significant variation in the physicochemical parameters at higher temperatures is attributed to the conglomeration of PPN-PCL-NPs due to polymer degradation.[36] From the finding, it was inferred that the developed PPN-PCL-NPs can be stored at ≤25 °C to retain the integrity of the nanocarriers.

**3.4. In-Vitro Drug Release Study.** The drug release behavior of PPN-PCL-NPs and the free PPN suspension was evaluated over a span of 48 h through the dialysis bag technique, employing a phosphate buffer pH 7.4 as release media at 37 ± 1 °C temperature. The calibration plot of PPN is shown in Figure S1. The time versus % cumulative drug release profile is depicted in Figure 7. The optimized PPN PCL-NPs displayed a biphasic release profile, with an initial burst release of 47.82 ± 3.92% within the initial 6 h interval, succeeded by a prolonged release extending over a duration of 48 h. This initial burst release was ascribed to drug molecules either adsorbed onto the surface or encapsulated within the outer core of the PPN-PCL-NPs. This phenomenon may also be ascribed to enhanced surface area due to the small PS of nanocarriers.[52] Following the rapid initial release, PPN-PCL-NPs demonstrated a controlled release

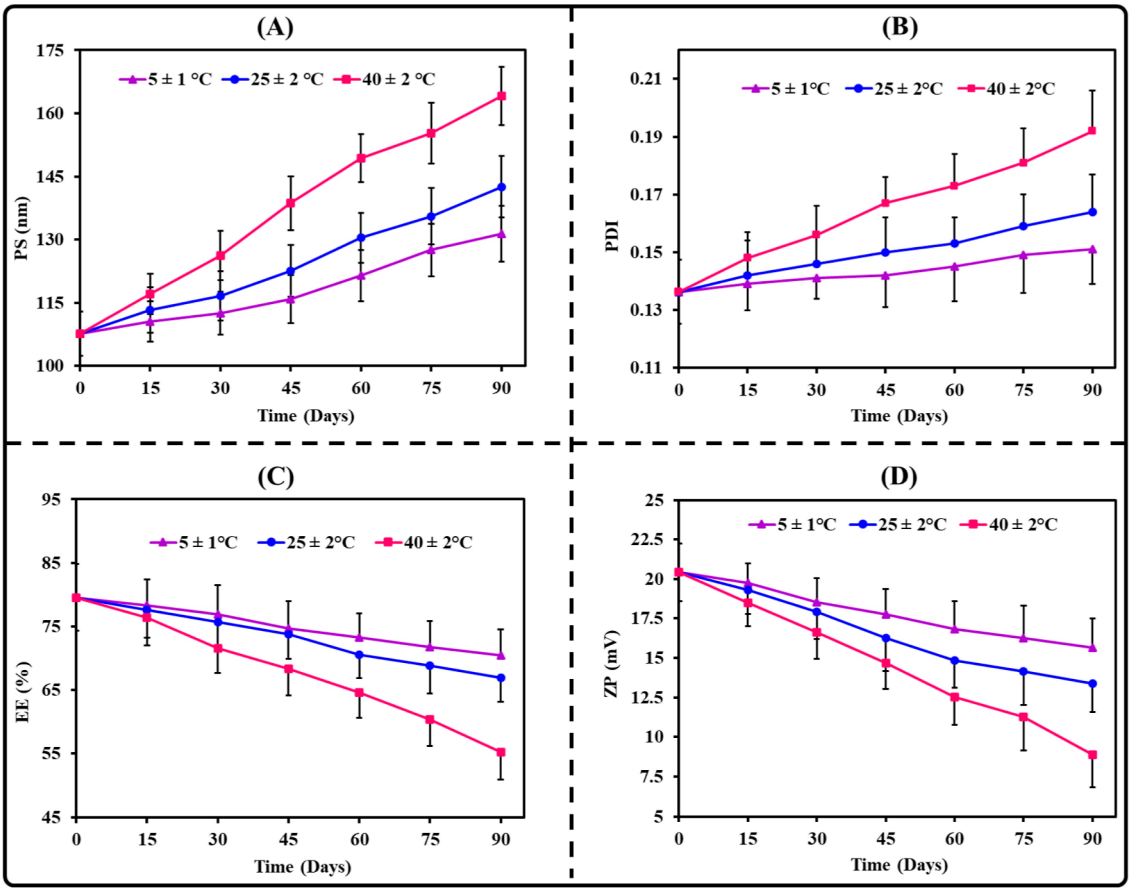


**Figure 6.** Plots representing the changes in different physicochemical parameters. (A) PS, (B) PDI, (C) % EE, and (D) ZP under different temperature conditions for 3 months.



https://doi.org/10.1021/acsomega.3c06605
ACS Omega 2023, 8, 44183−44194

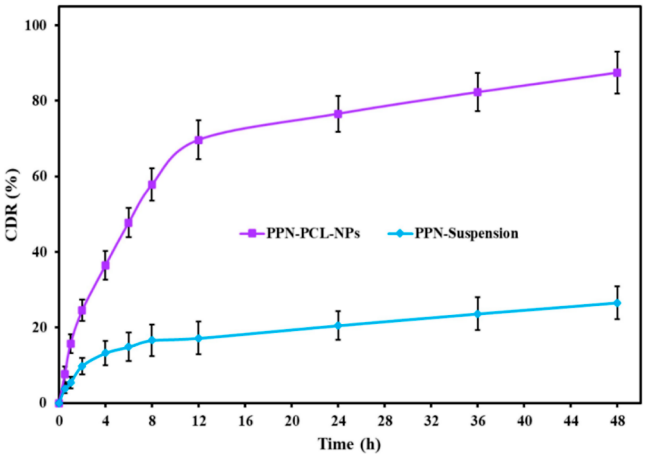


**Figure 7.** In vitro release profile of PPN-PCL-NPs and the PPN suspension.

profile. The extended release can be attributed to the process of drug diffusion originating from the inner core of the polymer matrix. Additionally, the slow and gradual diffusion of PPN from the lipophilic polymer matrix also contributed to a controlled drug release for an extended period.[36] Conversely, the free PPN suspension exhibited a 26.58 ± 4.37% release in 48 h. The limited dissolution of PPN from the suspension can be attributed to the limited solubility of the drug within the dissolution medium.

For the investigation of release kinetics, the drug release data set was fitted with various mathematical models, and the resultant outcomes are presented in Table 5. Upon comparative assessment of all models, the Korsmeyer−Peppas model was selected as the best-fitted mathematical model with the highest $R^2$ value, i.e., 0.9309. The release exponent "*n*" value ranged between 0 to 0.5, representing Fickian diffusion behavior. In the context of this study, the determined "*n*" value was found to be 0.223; thus, the PPN release mechanism from PCL-NPs follows the Fickian diffusion mechanism.[53]

**Table 5. Results of the Mechanism of Drug Release Kinetics from PPN-PCL-NPs after Fitting the Data into Different Mathematical Kinetic Models**

| model | model equation | $R^2$ | release exponent ("*n*") |
|---|---|---|---|
| zero order | $M_t = M_0 + k_0 t$ | 0.7328 | |
| first order | $\ln M_t = \ln M_0 + k_1 t$ | 0.9098 | |
| Higuchi matrix model | $M_t = M_0 + k t^{1/2}$ | 0.8962 | |
| Korsmeyer−Peppas model | $M_t/M_\infty = k t^n$ | 0.9309 | 0.223 |

**3.5. Cell Culture Experiment.** This experiment was conducted to investigate the therapeutic potential of PPN-PCL-NPs in the treatment of BC. The pharmaceutical attributes like the size and morphology of nanoparticles greatly affect the therapeutic efficacy. The nanoparticle with a small size (generally <200 nm) showed significantly higher cellular internalization and accumulation in the tumor microenvironment due to the EPR effect.[54,55] Smaller nanoparticles often have a larger surface area, which can lead to faster drug release in a controlled manner. Nanoparticles with spherical morphology showed the most favorable properties such as high surface-to-volume ratios for better therapeutic efficacy. Spherical nanoparticles exhibit significantly higher cellular uptake in cancer cells and prolong the circulation time in the body. These characteristics significantly increase the therapeutic efficacy of nanocarriers.[56,57] In this investigation, the in vitro cytotoxicity of free PPN and PPN-PCL-NPs was evaluated against MCF-7 breast tumor cells by the MTT assay. For evaluating the cytotoxicity of free PPN and PPN-PCL-NPs, MCF-7 cells were treated at various concentrations for different time periods, i.e., 24, 48, and 72 h. The results suggested a dose- and time-dependent cytotoxic effect against MCF-7 breast tumor cells as depicted in Figure 8. The optimized PPN-PCL-NPs exhibited much higher cytotoxicity at each concentration and time point compared to free PPN. A significant variation in the cytotoxicity was observed between free PPN and PPN-PCL-NPs. At all-time points, at a lower concentration, no significant variation in the results was observed. At the highest concentration of 100 μg/mL, PPN-PCL-NPs showed variable cell viabilities of 19.12 ± 2.9% (24 h), 10.23 ± 1.7% (48 h), and 5.73 ± 0.7% (72 h). In the case of free PPN, the cell viability was found to be 30.54 ± 3.2% (24 h), 23.62 ± 1.4% (48 h), and 16.98 ± 1.8% (72 h). The maximum significant difference was observed at 72 h with about a 3-fold increase in the activity for PPN-PCL-NPs. As time increased, the maximum PPN release from NPs showed a significant effect. There was a 2-fold enhancement in the activity observed at 48 and 72 h. So, from the results, we can say that the polymeric NPs are an ideal delivery system for cancer activity. The $IC_{50}$ values of free PPN and PPN-PCL-NPs against MCF-7 breast tumor cells at different time points are depicted in Figure 9. After 24 h of the treatment, the $IC_{50}$ values of free PPN and PPN-PCL-NPs were determined to be 55.81 ± 4.36 and 34.61 ± 3.13 μg/mL, respectively. After 48 h of treatment, the $IC_{50}$ value of free PPN and PPN-PCL-NPs was determined to be 35.88 ± 3.28 and 19.64 ± 2.49 μg/mL, respectively. After 72 h of treatment, the $IC_{50}$ values of free PPN and PPN-PCL-NPs were determined to be 21.73 ± 2.35 and 10.12 ± 2.18 μg/mL, respectively. The $IC_{50}$ value was found to be 1.6-fold at 24 h, 1.82-fold at 48 h, and 2.14-fold less than free PPN at each time point. The value of $IC_{50}$ was also found to be time-dependent. As time increased, the $IC_{50}$ value decreased. Much higher cytotoxicity with PPN-PCL-NPs was achieved due to sustained release and higher cellular internalization of the nanocarrier in the tumor cells. In addition, the greater cytotoxicity was attributed to small size, spherical morphology, and cytosolic PPN delivery from the nanocarrier.[38,39] Our finding also corroborated a previously published report. Kazmi et al. studied the anticancer effect of PPN-loaded polymeric nanoparticles on MCF-7 cells.[21] The researcher reported that the developed NPs showed $IC_{50}$ values of 21.32 ± 2.17 and 9.46 ± 2.18 μg/mL at 48 and 72 h, respectively. Therefore, it can be inferred that the development of PPN-encapsulated PCL-NPs can enhance the therapeutic efficacy against BC.

## 4. CONCLUSIONS

The present research seeks to investigate the potential of PPN-PCL-NPs as a potential strategy to enhance therapeutic outcomes in BC. Herein, the PPN-encapsulated PCL-NPs were successfully fabricated and optimized by $3^3$-BBD as well as characterized for different pharmaceutical attributes. The suggested 15 formulations were prepared according to the composition derived from the design and the values of responses were fitted to yield the optimized composition. The optimized formulation exhibits small PS (>150 nm) with excellent homogeneity and high % EE (~80%). The developed


https://doi.org/10.1021/acsomega.3c06605
ACS Omega 2023, 8, 44183−44194

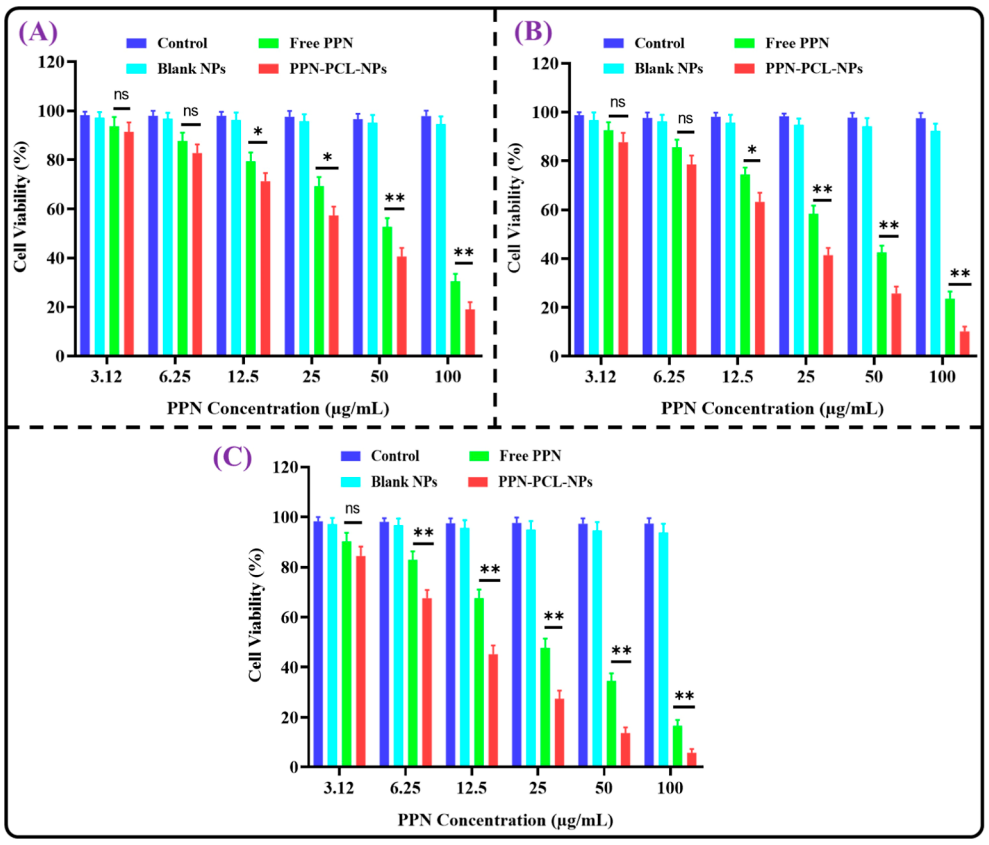


**Figure 8.** Plots representing the cell viability vs concentration profile of free PPN and PPN-PCL-NPs at (A) 24, (B) 48, and (C) 72 h against MCF-7 breast tumor cells.

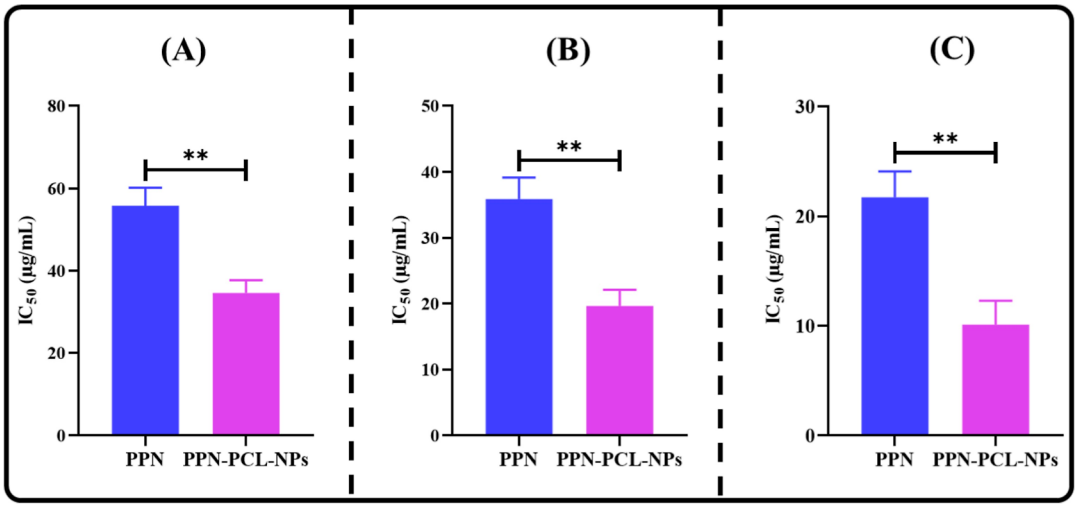


**Figure 9.** Plots representing the $IC_{50}$ values of free PPN and PPN-PCL-NPs at (A) 24, (B) 48, and (C) 72 h against MCF-7 breast tumor cells.

nanocarrier showed excellent stability and sustained release of the drug for 48 h. A dose- and time-dependent in vitro cytotoxicity was achieved from the developed PCL-NPs compared to the native PPN confirmed our hypothesis that it exhibits higher activity against the tested MCF 7 breast cancer cell line. Overall, the PCL-NPs provide a potential drug delivery platform to achieve optimal therapeutic efficacy against BC. Additionally, conducting in vivo experiments could provide valuable validation for the in vitro performance of the PCL-NPs.

## ■ ASSOCIATED CONTENT

### Supporting Information

The Supporting Information is available free of charge at https://pubs.acs.org/doi/10.1021/acsomega.3c06605.

Details of the analytical method, calibration plot of PPN over the concentration range used to calculate different parameters; and validation data (accuracy and precision) for the method used (PDF)



https://doi.org/10.1021/acsomega.3c06605
ACS Omega 2023, 8, 44183−44194

## AUTHOR INFORMATION


### Corresponding Author

**Sadaf Jamal Gilani** − *Department of Basic Health Sciences, Foundation Year, Princess Nourah Bint Abdulrahman University, Riyadh 11671, Saudi Arabia;* orcid.org/0000-0002-9590-3856; Email: SJGlani@pnu.edu.sa

### Authors

**May Nasser Bin-Jumah** − *Biology Department, College of Science and Environment and Biomaterial Unit, Health Sciences Research Center, Princess Nourah Bint Abdulrahman University, Riyadh 11671, Saudi Arabia; Saudi Society for Applied Science, Princess Nourah Bint Abdulrahman University, Riyadh 11671, Saudi Arabia*

**Farhat Fatima** − *Department of Pharmaceutics, College of Pharmacy, Prince Sattam Bin Abdulaziz University, Al-Kharj 11942, Saudi Arabia*

Complete contact information is available at: https://pubs.acs.org/10.1021/acsomega.3c06605


### Notes

The authors declare no competing financial interest.

## ACKNOWLEDGMENTS

This research project was supported by Princess Nourah bint Abdulrahman University Researchers Supporting Project number (PNURSP2023R108), Princess Nourah bint Abdulrahman University, Riyadh, Saudi Arabia.

## REFERENCES


(1) Rizwanullah, M.; Ahmad, M. Z.; Ghoneim, M. M.; Alshehri, S.; Imam, S. S.; Md, S.; Alhakamy, N. A.; Jain, K.; Ahmad, J. Receptor-Mediated Targeted Delivery of Surface-ModifiedNanomedicine in Breast Cancer: Recent Update and Challenges. *Pharmaceutics* **2021**, *13* (12), 2039.

(2) Sung, H.; Ferlay, J.; Siegel, R. L.; Laversanne, M.; Soerjomataram, I.; Jemal, A.; Bray, F. Global Cancer Statistics 2020: GLOBOCAN Estimates of Incidence and Mortality Worldwide for 36 Cancers in 185 Countries. *CA: Cancer J. Clin.* **2021**, *71* (3), 209−249.

(3) Dubey, S. K.; Bhatt, T.; Agrawal, M.; Saha, R. N.; Saraf, S.; Saraf, S.; Alexander, A. Application of Chitosan Modified Nanocarriers in Breast Cancer. *Int. J. Biol. Macromol.* **2022**, *194*, 521−538.

(4) Yang, B.; Song, B. P.; Shankar, S.; Guller, A.; Deng, W. Recent Advances in Liposome Formulations for Breast Cancer Therapeutics. *Cell. Mol. Life Sci.* **2021**, *78* (13), 5225−5243.

(5) Rizwanullah, M.; Perwez, A.; Alam, M.; Ahmad, S.; Mir, S. R.; Rizvi, M. M. A.; Amin, S. Polymer-Lipid Hybrid Nanoparticles of Exemestane for Improved Oral Bioavailability and Anti-Tumor Efficacy: An Extensive Preclinical Investigation. *Int. J. Pharm.* **2023**, *642*, 123136.

(6) Taghipour-Sabzevar, V.; Sharifi, T.; Moghaddam, M. M. Polymeric Nanoparticles as Carrier for Targeted and Controlled Delivery of Anticancer Agents. *Ther. Deliv.* **2019**, *10* (8), 527−550.

(7) Haq, I. U.; Imran, M.; Nadeem, M.; Tufail, T.; Gondal, T. A.; Mubarak, M. S. Piperine: A Review of Its Biological Effects. *Phytother Res.* **2021**, *35* (2), 680−700.

(8) Zadorozhna, M.; Tataranni, T.; Mangieri, D. Piperine: Role in Prevention and Progression of Cancer. *Mol. Biol. Rep.* **2019**, *46* (5), 5617−5629.

(9) Rather, R. A.; Bhagat, M. Cancer Chemoprevention and Piperine: Molecular Mechanisms and Therapeutic Opportunities. *Front. Cell Dev. Biol.* **2018**, *6* (FEB), 10.

(10) Manayi, A.; Nabavi, S. M.; Setzer, W. N.; Jafari, S. Piperine as a Potential Anti-Cancer Agent: A Review on Preclinical Studies. *Curr. Med. Chem.* **2019**, *25* (37), 4918−4928.

(11) Quijia, C. R.; Chorilli, M. Piperine for Treating Breast Cancer: A Review of Molecular Mechanisms, Combination with Anticancer Drugs, and Nanosystems. *Phytother Res.* **2022**, *36* (1), 147−163.

(12) Quijia, C. R.; Araujo, V. H.; Chorilli, M. Piperine: Chemical, Biological and Nanotechnological Applications. *Acta Pharm.* **2021**, *71* (2), 185−213.

(13) Ezawa, T.; Inoue, Y.; Murata, I.; Takao, K.; Sugita, Y.; Kanamoto, I. Characterization of the Dissolution Behavior of Piperine/Cyclodextrins Inclusion Complexes. *AAPS PharmSciTech* **2018**, *19* (2), 923−933.

(14) Suresh, D.; Srinivasan, K. Tissue Distribution & Elimination of Capsaicin, Piperine & Curcumin Following Oral Intake in Rats. *Indian J. Med. Res.* **2010**, *131* (5), 682−691.

(15) Huang, X. S. Determination of Equilibrium Solubility and Apparent Oil/Water Partition Coefficient of Piperine. *J. Jinan Univ.* **2012**, *5* (33), 473-476.

(16) Ren, T.; Hu, M.; Cheng, Y.; Shek, T. L.; Xiao, M.; Ho, N. J.; Zhang, C.; Leung, S. S. Y.; Zuo, Z. Piperine-Loaded Nanoparticles with Enhanced Dissolution and Oral Bioavailability for Epilepsy Control. *Eur. J. Pharm. Sci.* **2019**, *137*, 104988.

(17) Li, J.; Wu, T.; Li, S.; Chen, X.; Deng, Z.; Huang, Y. Nanoparticles for Cancer Therapy: A Review of Influencing Factors and Evaluation Methods for Biosafety. *Clin. Transl. Oncol.* **2023**, *25* (7), 2043−2055.

(18) Rizwanullah, M.; Amin, S.; Mir, S. R.; Fakhri, K. U.; Rizvi, M. M. A. Phytochemical Based Nanomedicines against Cancer: Current Status and Future Prospects. *J. Drug Target.* **2018**, *26* (9), 731−752.

(19) Shi, J.; Kantoff, P. W.; Wooster, R.; Farokhzad, O. C. Cancer Nanomedicine: Progress, Challenges and Opportunities. *Nat. Rev. Cancer* **2017**, *17* (1), 20−37.

(20) Pachauri, M.; Gupta, E. D.; Ghosh, P. C. Piperine Loaded PEG-PLGA Nanoparticles: Preparation, Characterization and Targeted Delivery for Adjuvant Breast Cancer Chemotherapy. *J. Drug Deliv. Sci. Technol.* **2015**, *29*, 269−282.

(21) Kazmi, I.; Al-Abbasi, F. A.; Imam, S. S.; Afzal, M.; Nadeem, M. S.; Altayb, H. N.; Alshehri, S. Formulation of Piperine Nanoparticles: In Vitro Breast Cancer Cell Line and In Vivo Evaluation. *Polymers* **2022**, *14* (7), 1349.

(22) Woodruff, M. A.; Hutmacher, D. W. The Return of a Forgotten Polymer—Polycaprolactone in the 21st Century. *Prog. Polym. Sci.* **2010**, *35* (10), 1217−1256.

(23) Li, Z.; Tan, B. H. Towards the Development of Polycaprolactone Based Amphiphilic Block Copolymers: Molecular Design, Self-Assembly and Biomedical Applications. *Mater. Sci. Eng., C* **2014**, *45*, 620−634.

(24) Dash, T. K.; Konkimalla, V. B. Poly-ϵ-Caprolactone Based Formulations for Drug Delivery and Tissue Engineering: A Review. *J. Controlled Release* **2012**, *158* (1), 15−33.

(25) Sisson, A. L.; Ekinci, D.; Lendlein, A. The Contemporary Role of ε-Caprolactone Chemistry to Create Advanced Polymer Architectures. *Polymer* **2013**, *54* (17), 4333−4350.

(26) Almeida, M.; Magalhães, M.; Veiga, F.; Figueiras, A. Poloxamers, Poloxamines and Polymeric Micelles: Definition, Structure and Therapeutic Applications in Cancer. *J. Polym. Res.* **2018**, *25* (1), 31.

(27) Zarrintaj, P.; Ramsey, J. D.; Samadi, A.; Atoufi, Z.; Yazdi, M. K.; Ganjali, M. R.; Amirabad, L. M.; Zangene, E.; Farokhi, M.; Formela, K.; Saeb, M. R.; Mozafari, M.; Thomas, S. Poloxamer: A Versatile Tri-Block Copolymer for Biomedical Applications. *Acta Biomater.* **2020**, *110*, 37−67.

(28) Bollenbach, L.; Buske, J.; Mäder, K.; Garidel, P. Poloxamer 188 as Surfactant in Biological Formulations - An Alternative for Polysorbate 20/80? *Int. J. Pharm.* **2022**, *620*, 121706.

(29) de Oliveira Junior, E. R.; Nascimento, T. L.; Salomão, M. A.; da Silva, A. C. G.; Valadares, M. C.; Lima, E. M. Increased Nose-to-Brain Delivery of Melatonin Mediated by Polycaprolactone Nanoparticles for the Treatment of Glioblastoma. *Pharm. Res.* **2019**, *36* (9), 131.

(30) Crucho, C. I. C.; Barros, M. T. Polymeric Nanoparticles: A Study on the Preparation Variables and Characterization Methods. *Mater. Sci. Eng., C* **2017**, *80*, 771−784.

(31) Badri, W.; Miladi, K.; Robin, S.; Viennet, C.; Nazari, Q. A.; Agusti, G.; Fessi, H.; Elaissari, A. Polycaprolactone Based Nanoparticles Loaded with Indomethacin for Anti-Inflammatory Therapy: From Preparation to Ex Vivo Study. *Pharm. Res.* **2017**, *34* (9), 1773−1783.
(32) Sarkar, P.; Bhattacharya, S.; Pal, T. K. Application of Statistical Design to Evaluate Critical Process Parameters and Optimize Formulation Technique of Polymeric Nanoparticles. *R. Soc. Open Sci.* **2019**, *6* (7), 190896.
(33) Zanetti, M.; Mazon, L. R.; de Meneses, A. C.; Silva, L. L.; de Araújo, P. H. H.; Fiori, M. A.; de Oliveira, D. Encapsulation of Geranyl Cinnamate in Polycaprolactone Nanoparticles. *Mater. Sci. Eng., C* **2019**, *97*, 198−207.
(34) Badri, W.; El Asbahani, A.; Miladi, K.; Baraket, A.; Agusti, G.; Nazari, Q. A.; Errachid, A.; Fessi, H.; Elaissari, A. Poly (ε-Caprolactone) Nanoparticles Loaded with Indomethacin and Nigella Sativa L. Essential Oil for the Topical Treatment of Inflammation. *J. Drug Deliv. Sci. Technol.* **2018**, *46*, 234−242.
(35) Xu, C.; Li, S.; Chen, J.; Wang, H.; Li, Z.; Deng, Q.; Li, J.; Wang, X.; Xiong, Y.; Zhang, Z.; Yang, X.; Li, Z. Doxorubicin and Erastin Co-Loaded Hydroxyethyl Starch-Polycaprolactone Nanoparticles for Synergistic Cancer Therapy. *J. Controlled Release* **2023**, *356*, 256−271.
(36) Khan, S.; Aamir, M. N.; Madni, A.; Jan, N.; Khan, A.; Jabar, A.; Shah, H.; Rahim, M. A.; Ali, A. Lipid Poly (ε-Caprolactone) Hybrid Nanoparticles of 5-Fluorouracil for Sustained Release and Enhanced Anticancer Efficacy. *Life Sci.* **2021**, *284*, 119909.
(37) Kumar, A.; Sawant, K. Encapsulation of Exemestane in Polycaprolactone Nanoparticles: Optimization, Characterization, and Release Kinetics. *Cancer Nanotechnol.* **2013**, *4* (4−5), 57−71.
(38) Rizwanullah, M.; Perwez, A.; Mir, S. R.; Alam Rizvi, M. M.; Amin, S. Exemestane Encapsulated Polymer-Lipid Hybrid Nanoparticles for Improved Efficacy against Breast Cancer: Optimization, in Vitro Characterization and Cell Culture Studies. *Nanotechnology* **2021**, *32* (41), 415101.
(39) Kazmi, I.; Al-Abbasi, F. A.; Imam, S. S.; Afzal, M.; Nadeem, M. S.; Altayb, H. N.; Alshehri, S. Formulation and Evaluation of Apigenin-Loaded Hybrid Nanoparticles. *Pharmaceutics* **2022**, *14* (4), 783.
(40) Snehalatha, M.; Venugopal, K.; Saha, R. N. Etoposide-Loaded PLGA and PCL Nanoparticles I: Preparation and Effect of Formulation Variables. *Drug Deliv.* **2008**, *15* (5), 267−275.
(41) Diwan, R.; Ravi, P. R.; Agarwal, S. I.; Aggarwal, V. Cilnidipine Loaded Poly (ε-Caprolactone) Nanoparticles for Enhanced Oral Delivery: Optimization Using DoE, Physical Characterization, Pharmacokinetic, and Pharmacodynamic Evaluation. *Pharm. Dev. Technol.* **2021**, *26* (3), 278−290.
(42) Sharma, N.; Madan, P.; Lin, S. Effect of Process and Formulation Variables on the Preparation of Parenteral Paclitaxel-Loaded Biodegradable Polymeric Nanoparticles: A Co-Surfactant Study. *Asian J. Pharm. Sci.* **2016**, *11* (3), 404−416.
(43) Gajra, B.; Dalwadi, C.; Patel, R. Formulation and Optimization of Itraconazole Polymeric Lipid Hybrid Nanoparticles (Lipomer) Using Box Behnken Design. *Daru, J. Pharm. Sci.* **2015**, *23* (1), 3.
(44) Nawaz, T.; Iqbal, M.; Khan, B. A.; Nawaz, A.; Hussain, T.; Hosny, K. M.; Abualsunun, W. A.; Rizg, W. Y. Development and Optimization of Acriflavine-Loaded Polycaprolactone Nanoparticles Using Box-Behnken Design for Burn Wound Healing Applications. *Polymers* **2021**, *14* (1), 101.
(45) Singh, Y.; Ojha, P.; Srivastava, M.; Chourasia, M. K. Reinvestigating Nanoprecipitation via Box-Behnken Design: A Systematic Approach. *J. Microencapsul.* **2015**, *32* (1), 75−85.
(46) Abriata, J. P.; Turatti, R. C.; Luiz, M. T.; Raspantini, G. L.; Tofani, L. B.; do Amaral, R. L. F.; Swiech, K.; Marcato, P. D.; Marchetti, J. M. Development, Characterization and Biological in Vitro Assays of Paclitaxel-Loaded PCL Polymeric Nanoparticles. *Mater. Sci. Eng., C* **2019**, *96*, 347−355.
(47) Wong, C. Y.; Martinez, J.; Zhao, J.; Al-Salami, H.; Dass, C. R. Development of Orally Administered Insulin-Loaded Polymeric-Oligonucleotide Nanoparticles: Statistical Optimization and Physicochemical Characterization. *Drug Dev. Ind. Pharm.* **2020**, *46* (8), 1238−1252.
(48) Kang, H.; Rho, S.; Stiles, W. R.; Hu, S.; Baek, Y.; Hwang, D. W.; Kashiwagi, S.; Kim, M. S.; Choi, H. S. Size-Dependent EPR Effect of Polymeric Nanoparticles on Tumor Targeting. *Adv. Healthcare Mater.* **2020**, *9* (1), 1901223.
(49) Lazzari, S.; Moscatelli, D.; Codari, F.; Salmona, M.; Morbidelli, M.; Diomede, L. Colloidal Stability of Polymeric Nanoparticles in Biological Fluids. *J. Nanopart. Res.* **2012**, *14* (6), 920.
(50) Zein, R.; Sharrouf, W.; Selting, K. Physical Properties of Nanoparticles That Result in Improved Cancer Targeting. *J. Oncol* **2020**, *2020*, 1−16.
(51) Gagliardi, A.; Giuliano, E.; Venkateswararao, E.; Fresta, M.; Bulotta, S.; Awasthi, V.; Cosco, D. Biodegradable Polymeric Nanoparticles for Drug Delivery to Solid Tumors. *Front. Pharmacol* **2021**, *12*, 601626.
(52) Lin, X.; Wang, Q.; Du, S.; Guan, Y.; Qiu, J.; Chen, X.; Yuan, D.; Chen, T. Nanoparticles for Co-Delivery of Paclitaxel and Curcumin to Overcome Chemoresistance against BC. *J. Drug Deliv. Sci. Technol.* **2023**, *79*, 104050.
(53) Dash, S.; Murthy, P.; Nath, L.; Chowdhury, P. Kinetic Modeling on Drug Release from Controlled Drug Delivery Systems. *Acta Polym. Pharm.* **2010**, *67* (3), 217−223.
(54) Tay, C. Y.; Setyawati, M. I.; Xie, J.; Parak, W. J.; Leong, D. T. Back to Basics: Exploiting the Innate Physico-Chemical Characteristics of Nanomaterials for Biomedical Applications. *Adv. Funct. Mater.* **2014**, *24* (38), 5936−5955.
(55) Salatin, S.; Maleki Dizaj, S.; Yari Khosroushahi, A. Effect of the Surface Modification, Size, and Shape on Cellular Uptake of Nanoparticles. *Cell Biol. Int.* **2015**, *39* (8), 881−890.
(56) Duan, X.; Li, Y. Physicochemical Characteristics of Nanoparticles Affect Circulation, Biodistribution, Cellular Internalization, and Trafficking. *Small* **2013**, *9* (9−10), 1521−1532.
(57) Zhao, Z.; Ukidve, A.; Krishnan, V.; Mitragotri, S. Effect of Physicochemical and Surface Properties on in Vivo Fate of Drug Nanocarriers. *Adv. Drug Delivery Rev.* **2019**, *143*, 3−21.


https://doi.org/10.1021/acsomega.3c06605
*ACS Omega* 2023, 8, 44183−44194